Title

Isolation of neutralizing monoclonal antibodies to human astrovirus and characterization of virus variants that escape neutralization

Journal

Journal of Virology, 93(2)

ISSN

0022-538X

Authors

Espinosa, Rafaela
López, Tomás
Bogdanoff, Walter A
et al.

Publication Date

2019-01-15

DOI

10.1128/jvi.01465-18

Peer reviewed

Isolation of neutralizing monoclonal antibodies to human astrovirus and characterization of virus variants that escape neutralization

Rafaela Espinosa[a*], Tomás López[a*], Walter A. Bogdanoff[b], Marco A. Espinoza[a], Susana López[a], Rebecca M. DuBois[b], and Carlos F. Arias[a#]

[a]Departamento de Genética del Desarrollo y Fisiología Molecular, Instituto de Biotecnología, Universidad Nacional Autónoma de México, Cuernavaca, Morelos, México. [b]Department of Biomolecular Engineering, University of California Santa Cruz, Santa Cruz, California, USA

Running Head: Antigenic structure of human astroviruses

[#]Address correspondence to Carlos F. Arias, arias@ibt.unam.mx

[*]These two authors contributed equally to this work

Key words: astrovirus, neutralizing antibodies, astrovirus antigenic structure

Word counts

Abstract: 250

Text: 4,468

ABSTRACT

Human astroviruses (HAstVs) cause severe diarrhea and represent an important health problem in children under two years of age. Despite their medical importance, the study of these pathogens has been neglected. To better understand the astrovirus antigenic structure and the basis of protective immunity, in this work we produced a panel of neutralizing monoclonal antibodies (Nt-MAbs) to HAstV serotypes 1, 2, and 8, and identified the mutations that allow the viruses to escape neutralization. We first tested the capacity of the recombinant HAstV capsid core and spike domains to elicit Nt-Ab. Hyperimmunization of animals with the two domains showed that although both induced a potent immune response, only the spike was able to elicit antibodies with neutralizing activity. Based on this finding, we used a mixture of the recombinant spike domains belonging to the three HAstV serotypes to immunize mice. Five Nt-MAbs were isolated and characterized; all of them were serotype-specific, two were directed to HAstV-1, one to HAstV-2, and two to HAstV-8. These antibodies were used to select single and double neutralization-escape variant viruses, and determination of the amino acid changes that allow the viruses to escape neutralization permitted us to define the existence of four potentially independent neutralization epitopes on the HAstV capsid. These studies provide the basis for development of subunit vaccines that induce neutralizing antibodies, and tools to explore the possibility to develop a specific antibody therapy for astrovirus disease. Our results also establish a platform to advance our knowledge on HAstV cell binding and entry.

Relevance

Human astroviruses (HAstVs) are common etiological agents of acute gastroenteritis in children, the elderly, and immunocompromised patients; some virus strains have also been associated with neurological disease. Despite their medical importance, the study of these pathogens has advanced at a slow pace. In this work, we produced neutralizing antibodies to the virus and mapped the epitopes they recognize on the virus capsid. These studies provide the basis for development of subunit vaccines that induce neutralizing antibodies, as well as tools to explore the development of a specific antibody therapy for astrovirus disease. Our results also establish a platform to advance our knowledge on HAstV cell binding and entry.

Introduction

Human astroviruses (HAstVs) are common etiological agents of acute gastroenteritis in children, the elderly, and immunocompromised patients (1-3). They are estimated to be responsible for 2 to 9% acute, nonbacterial childhood diarrhea (4). Recently, the epidemiology of HAstV in community settings of 8 low- and middle-income countries with high prevalence of diarrhea and undernutrition was reported (5); the prevalence of HAstV in diarrheal stools was 5.6%, and remarkably, its severity exceeded all enteropathogens tested, except rotavirus. In a related study, norovirus GII, rotavirus, and astrovirus exhibited the highest attributable burdens of diarrhea in the first two years of life (6). These studies show that HAstV is an overlooked cause of diarrhea among vulnerable children worldwide, and they highlight the need for future research as well as the importance of this virus as a target for vaccine development (5, 6).

HAstVs are classified into 8 classical serotypes (HAstV-1 to -8) associated with acute gastroenteritis, however novel HAstV strains have been recently described and are also associated with neurological disease, including meningitis and encephalitis in immunocompromised patients (4). HAstVs are small, nonenveloped viruses with a single-stranded positive-sense RNA genome of about 6.8 kb comprising three open reading frames (ORFs). ORF2 encodes a capsid precursor structural polyprotein of about 90 kDa that self-assembles intracellularly and is processed by caspases to produce a virus particle formed by a 70 kDa protein (VP70) (7). This immature particle egresses the cell and is further processed by extracellular proteases; *in vitro*, the treatment of this particle with trypsin yields a mature infectious virus that, in HAstV-8, contains three

79 protein species of approximately 34 (VP34), 27 (VP27), and 25 (VP25) kDa (7), although
80 it has been recently shown that only VP34 and VP27 are relevant for HAstV-8 infectivity
81 (8).

82 Cryo-electron microscopy of mature HAstV virions reveals particles of 44 nm
83 comprised of a T=3 icosahedral shell and 30 globular spikes (9). The crystal structures of
84 both VP34 (10, 11) and VP25 (11-14) have been recently determined; VP34 folds into a
85 domain that constitutes the shell of the virus capsid (core domain), while VP27/VP25
86 form dimeric capsid spikes (spike domain). VP34 is derived from the highly conserved N-
87 terminal region of VP70, while VP27/VP25, which differ only at their amino terminus,
88 are derived from the hypervariable region of VP70 (15). Despite important advances in
89 the structural characterization of the HAstV particle, the functional sites on the virus
90 capsid, including the location of the receptor-binding site and the antigenic
91 determinants where neutralizing antibodies bind, have been poorly characterized. Only
92 one neutralizing antibody epitope, located on the capsid spike domain, has previously
93 been defined by X-ray crystallography (12).

94 To better understand the astrovirus antigenic structure and the basis of
95 protective immunity, in this work we produced neutralizing monoclonal antibodies (Nt-
96 MAbs) to HAstV serotypes 1, 2, and 8 and identified the mutations that allow variant
97 viruses to escape neutralization. This allowed us to define the existence of four
98 potentially independent neutralization epitopes on the HAstV capsid. These studies
99 provide the basis for the development of subunit vaccines to induce neutralizing
100 antibodies and tools to explore the possibility to develop a specific antibody therapy for

101 astrovirus disease. Our results also establish a platform to advance our knowledge on
102 HAstV cell binding and entry.
103
104 **RESULTS**
105 **The HAstV capsid spike but not the capsid core domain induces neutralizing**
106 **antibodies.** To identify the neutralization epitopes on the HAstV capsid, we first
107 evaluated the capacity of the core and spike domains to induce total (ELISA) and
108 neutralizing antibodies. These two structural domains of the virus can be produced in *E.*
109 *coli* in a soluble and correctly folded form (10-14). Rabbits and mice were immunized
110 with either the purified, recombinant core or the spike domains of HAstV-1 (core1 or
111 spike1). As expected, both domains were immunogenic and induced a robust antibody
112 response (Fig. 1A). We then tested the capacity of the polyclonal sera directed to either
113 domain to neutralize the infectivity of HAstV-1. The core1 did not induce a detectable
114 level of neutralizing antibodies to either HAstV-1, HAstV-2 or HAstV-8 (Fig. 1B), while the
115 spike1 domain induced a high (>1/50,000) neutralizing response that was specific for
116 HAstV-1 (Fig. 1B)
117 Of interest, despite the fact that the anti-spike1 mouse polyclonal serum (both
118 rabbit and mice sera behaved equally in all assays tested) was specific for HAstV-1 by
119 neutralization, it also recognized the heterologous capsid spikes of HAstV-2 and -8
120 (spike2 and spike8) by ELISA, although about 50 to 100 times less efficiently (Fig. 2A).
121 The anti-spike2 antibodies (see Material and Methods) interacted also weaker with
122 spikes 1 and 8 (Fig. 2B). On the other hand, the anti-spike8 serum recognized better the

123 spike1 (with about 5 to 10-fold difference) than the spike2, which was bound about 100
124 times less efficiently (Fig. 2C). In turn, the anti-core1 polyclonal serum cross-reacted
125 efficiently with the core domain of both HAstV-2 and HAstV-8 by Western blot, and also
126 recognized cells infected with HAstV serotypes 1, 2, or 8, by both immunocytochemistry
127 and immunofluorescence (Figs. 2D and 2E).
128
129 **Isolation and serotype-specificity of neutralizing monoclonal antibodies.** Given that the
130 spike was the only domain that induced neutralizing antibodies, we used it to immunize
131 mice to generate Nt-MAbs. Since we were interested in isolating cross-reactive,
132 heterotypic Nt-MAbs, we immunized mice with a mixture of spike domains of HAstV
133 serotypes 1, 2, and 8, following the immunization scheme described in Material and
134 Methods. The primary screening for hybridomas secreting astrovirus-specific MAbs was
135 carried out by ELISA, using as antigens the individual spike proteins from the three
136 different HAstV serotypes. We selected 54 positives hybridomas from 480 wells initially
137 screened; twenty-one for spike1, one for spike 2, and sixteen for spike8. Thirteen were
138 cross-reactive with at least 2 serotypes, and three recognized the spike domain of the 3
139 serotypes. Twenty-two of these hybridomas were further screened by a neutralization
140 assay. Twelve of these MAbs had neutralizing activity, and five of them that grew stably
141 were cloned and expanded for further analysis. Of these, two Nt-MAbs were directed to
142 HAstV-1 (MAbs 3B4 and 3H4), one to HAstV-2 (MAb 4B6), and two to HAstV-8 (MAbs
143 2D9 and 3E8). All five Nt-MAbs were serotype-specific by ELISA (not shown) and

144 neutralization (Fig. 3), and also specifically recognized their antigen by
145 immunocytochemistry and immunofluorescence in Caco-2 infected cells (not shown).
146 In general, all selected MAbs neutralized the cognate virus to high titers. Those
147 specific for HAstV-1 had a neutralization titer higher than 1/10,000, which was slightly
148 lower than the neutralization titer achieved with the hyperimmune polyclonal serum to
149 spike1 (Table 1, and Figs. 3A, 3B, and 3F); MAb 4B6, directed to HAstV-2, had a
150 neutralization titer of more than 1/100,000, similar to that of the hyperimmune
151 polyclonal serum to spike2 (Table 1, and Figs. 3C and 3F); MAbs 2D9 and 3E8, directed to
152 HAstV-8, reached a neutralization titer of more than one million, a titer about 10 to 50-
153 fold higher than that reached with the polyclonal antibodies to spike8 (Table 1, and
154 Figs. 3D, 3E, and 3F).
155
156 **Isolation of virus variants resistant to neutralization by monoclonal antibodies**. To
157 determine the immunogenic topology of the viral capsid, we selected virus variants
158 resistant to neutralization by each of the five MAbs characterized. Each neutralization-
159 escape variant was completely resistant to the corresponding Nt-MAb even at a 10^{-3}
160 dilution of the ascites fluid (Fig. 4), with exception of the escape variant for MAb 2D9
161 (vHAstV-8/2D9), which was slightly neutralized by MAb 2D9 (titer 5 x 10^{-3}) (Fig. 4D),
162 although more than 1,000-fold less efficiently as compared to the wt HAstV-8 virus (titer
163 8 x 10^{-6}) (see Fig. 4D). On the other hand, all escape variants were still efficiently
164 neutralized by the corresponding hyperimmune anti-spike serum (Fig. 4), indicating the
165 existence of more than one neutralization epitope on the spike domain of HAstV.

When cross-neutralization of escape variants of the same HAstV serotype were tested, i.e., neutralization of vHAstV-1/3B4 by MAb 3H4 and neutralization of vHAstV-1/3H4 by MAb 3B4, an efficient inhibition of infectivity was still observed, suggesting that the these two MAbs recognize two different epitopes on the virus (Figs. 4A and 4B). Similar results were obtained when HAstV-8 neutralization-escape variants vHAstV-8/2D9 and vHAstV-8/3E8 were evaluated for inhibition by MAbs 2D9 and 3E8, since they were neutralized with titers higher than 10^{-6} by the "non-homologous" MAb, suggesting again that these MAbs might interact with two different antigenic determinants on the HAstV-8 capsid (Figs. 4D and 4E). Of interest, it was also possible to isolate HAstV-1 variants that were highly resistant to neutralization by both MAbs 3B4 and 3H4, as well as HAstV-8 double-escape variants that were resistant to inhibition by both 2D9 and 3E8 MAbs (Fig. 5), showing the resilience of the virus to withstand mutations in more than one site in order to escape antibody neutralization. Even more, the double-escape variants were still efficiently neutralized by the hyperimmune polyclonal sera, suggesting that there are more than two neutralizing antigenic regions on the virus.

Identification of the amino acid changes that confer viruses resistance to neutralization by monoclonal antibodies. To understand the localization of the neutralization epitopes, we sequenced the genome region encoding the spike of the virus escape variants and identified amino acids changes that confer virus resistance to the Nt-MAbs. A single amino acid change was identified in the spike sequence of each single variant, with exception of vHAstV-2/4B6 that had two contiguous amino acids

changed (Table 2, Fig. 6A). The identified neutralization-escape mutations were then mapped onto the crystal structure of the spike1 domain (11); all of the mutated amino acids were located on the surface of the spike (Fig. 6B). In agreement with the results described above that suggest that the MAbs to HAstV-1 recognize different antigenic sites (Fig. 4), the amino acid residues that confer HAstV-1 resistance to neutralization by MAbs 3H4 and 3B4 were located into two very different regions of the spike (Fig. 6B, Table 2). A K504E change, located in loop 2, on the inferior/lateral region of the spike, conferred resistance to MAb 3H4, while the S560P mutation that results in the loss of neutralization by MAb 3B4, is located on the top of the spike in the middle of the long loop 3 that extends over the top, adjacent to the monomer-monomer contact in the spike, away from the K504E amino acid change.

The escape of neutralization of HAstV-2 by MAb 4B6 was the consequence of two contiguous amino acid changes (D564E, N565D) located in loop 3, on the top of the spike, very close to the amino acid that defines the resistance of HAstV-1 to MAb 3B4 (Fig. 6, Table 2). In the case of HAstV-8, the mutations that confer resistance to MAbs 3E8 and 2D9 were found to map on different sides of the spike, opposite to the dimeric subunit. These changes, Y464H for MAb 3E8 and D597Y for MAb 2D9 (Fig. 6, Table 2) are located, respectively, at the end of the large loop 1 and at the beginning of loop 4, and they may represent two independent epitopes.

Sequence analysis of the double-escape variants of HAstV-1 (vHAstV-1/3H4/3B4 and vHAstV-1/3B4/3H4) confirmed the mutations of the single-escape variants, bearing in both cases the two mutations identified individually in vHAstV-1/3H4 and vHAstV-

1/3B4 (Table 2). A similar finding was obtained when the double-escape variants of HAstV-8 were characterized (Table 2).

DISCUSSION

To gain insight into the antigenic sites of the HAstV capsid, Nt-MAbs directed to serotypes 1, 2, and 8 were produced, and the sites of amino acid mutations that allow the viruses to escape neutralization were mapped onto the virus capsid spike. Only two reports published over twenty years ago have described the isolation of Nt-MAbs to HAstV. In the first study, one MAb specific for HAstV-2 (MAb PL-2) was isolated (16). In the second work, three Nt-MAbs targeting HAstV-1 were reported (17). Despite the fact that in those studies purified virus was used as immunogen, all neutralizing MAbs isolated were directed to the spike domain, in agreement with our findings that the spike, but not the core domain is able to induce Nt-MAbs. Also, the crystal structure of the HAstV-2 spike bound to the Fab fragment of MAb PL-2 was recently reported (12), confirming the spike domain as a target for neutralizing antibodies. In the work by Bass et al. (17), the three MAbs to HAstV-1 were found to be topographically in close proximity, by a competition ELISA. All four Nt-MAbs previously reported were able to prevent the attachment of the virus particles to Caco-2 cells, suggesting that the spike domain also contains the receptor-binding site of the virion. These results indicate that a subunit vaccine should focus on the spike domain as the main immunogen to induce a potential protective antibody response.

231 Of interest, two of the Nt-MAb reported by Bass et al (17) neutralized more than
232 one serotype, with one of them being broadly neutralizing to all seven HAstV tested,
233 although this MAb was of IgM isotype and it probably was of low affinity. None of these
234 MAbs are currently available. In this regard, we found that about 1 out of 4 of the
235 initially positive hybridomas neutralized more than one serotype, indicating again the
236 existence of cross-neutralizing epitopes in the spike domain. It cannot be discarded,
237 however, that a proportion of the cross-reacting hybridomas were the result of a
238 mixture of two or more independent hybridoma cell clones having different serotype
239 specificity. Regardless of this fact, the cross-neutralization epitopes do not seem to be
240 immunodominant, at least in mice, since the anti-spike1 hyperimmune polyclonal serum
241 was serotype-specific by neutralization and recognized about 10-fold less efficiently the
242 HAstV-2 and HAstV-8 spikes by ELISA.
243 It is important to note that the infectivity of the neutralization-escape variants
244 was blocked by the hyperimmune serum to the corresponding spike to a titer similar to
245 that found for the wild-type virus. It would be interesting to test whether the
246 neutralization-escape variants are also efficiently neutralized or not by convalescent
247 sera from patients naturally infected with astrovirus, since in the case of rotavirus it has
248 been shown that marked differences can characterize the immune responses to
249 parenteral hyperimmunization in comparison with responses to intestinal infection (18).
250 Analysis of the structure of the recombinant HAstV-2 spike domain bound to scFv
251 PL-2 (12) showed that this neutralizing MAb recognizes a quaternary epitope on each
252 side of the dimeric capsid spike, and a deletion of three amino acids (aa 460-462) in

253 loop1 abolished the binding of PL-2. The location of the MAb3E8 escape mutation in
254 loop1 suggests that MAb 3E8 (anti-HAstV-8) may recognize an epitope that overlaps
255 with the MAb PL-2 (anti-HAstV-2), suggesting in turn that different HAstV serotypes may
256 share neutralization epitopes on the spike domain. In this regard, the escape mutations
257 that allow HAstV-1 and HAstV-2 to escape neutralization by MAbs 3B4 and 4B6,
258 respectively, are only 4 amino acids apart in loop 3 (see Table 2 and Fig. 6), suggesting
259 again that potentially this could be the same epitope shared by these two HAstV
260 serotypes. On the other hand, MAbs 3H4 and 2D9, localized in loops 2 and 4,
261 respectively, seem to define two new independent epitopes on the astrovirus capsid,
262 not previously reported. It is important to keep in mind that the amino acid changes
263 identified in the neutralization escape variants only represent mutations that allow the
264 virus to escape neutralization, and that they are not necessarily located in the epitope
265 recognized by the Nt-MAb, since distal mutations can, in principle, alter antibody
266 binding. Thus, in this work we have defined the potential existence of 4 different
267 neutralization epitopes on the astrovirus capsid, although some overlapping or indirect
268 effects of escape variants among them cannot be discarded.

269 Several patches of highly conserved amino acids among the eight HAstV
270 serotypes, conformed by amino acids that are distant in the linear sequence of the
271 spike, have been identified (12, 13); they have been proposed to represent potential
272 functional sites on the virus surface, including the so far unknown receptor binding site.
273 Of interest, all of the neutralizing escape mutations identified in this work, with
274 exception of K504E (vHAstV-1/3H4), map close (only between 5 and 10 amino acids

away) to the conserved amino acids that have been proposed to line the P and S sites, which are potentially functional sites identified in the HAstV-8 spike (13). It is likely that the footprint of the MAbs that recognized these epitopes overlaps the proposed functional P and S sites. Also, the footprint of MAb PL-2 on the HAstV2 spike was described to overlap four conserved amino acid regions, and to block the binding of the recombinant spike2 to Caco-2 cells, suggesting that this MAb could also inhibit the attachment of the virus to the cell surface through interfering the interaction of the virus with the cell receptor (12).

When screening the Genbank database to look for wildtype viruses that could have the mutations identified in our neutralization escape mutants, we found 24, 9, and 3 complete spike sequences that were annotated as HAstV serotypes 1, 2, or 8, respectively. None of the 24 HAstV-1 strains found had a change at Ser-560. In contrast the Lys-504 was only present in only one of the 24 viruses; one additional virus had a Pro in that position and twenty-two showed a Gln. Regarding HAstV-2, four of the spike sequences found showed Asp-Asn-Asn at amino acid positions 564-566, as the wildtype HAstV-2 virus characterized in this work, while five had a deletion of one of the two Asn residues. Finally, the three additional serotype 8 HAstV strains had the same amino acids as the parental Yuc8 virus at the amino acid residue positions where escape mutations to MAbs 2D9 and 3E8 were mapped. Overall, the finding of amino acid differences at some of the positions that allow our variant viruses to escape neutralization by the selected MAbs has to be interpreted cautiously, and cannot be ascribed to have occurred as the consequence of selective pressure in humans, since our

297 MAbs recognizes a mouse epitope, which could or could not be immunogenic in
298 humans. Whether these amino acid changes actually allow them to escape
299 neutralization by the MAbs described in this study needs to be determined

300 Work in progress in our labs is directed to define the mechanism of
301 neutralization of the antibodies characterized in this work, and to use structural biology
302 to define the antigenic sites of the Nt-MAbs described in this study. Altogether, our
303 results advance our knowledge on the antigenic structure of HAstVs, the basis of HAstV
304 neutralization, and the functional sites relevant for virus entry, providing a basis for the
305 development of vaccines and therapeutic measures against astrovirus disease.

306

307 **MATERIAL AND METHODS**

308 **Cells and viruses.** Caco-2 cells, clone C2Bbe1 (ATCC), were propagated in Dulbecco´s
309 modified Eagle´s medium-High Glucose (DMEM-HG) (Sigma) supplemented with non-
310 essential amino acids (Gibco) and 15% fetal bovine serum (FBS) (Cansera) in a 10% CO_2
311 atmosphere at 37°C. HAstV serotype 1 (HAstV-1-RIVMb) was obtained from Susana Guix
312 (Department de Microbiologia, Facultat de Biologia, Universitat de Barcelona, HAstV
313 serotype 2 strain Oxford (HAstV-2-Oxford) was obtained from J.B. Kurtz (Dept. of
314 Virology, John Radcliffe Hospital, Oxford, UK). HAstV serotype 8 strain Yuc8 was isolated
315 in our laboratory. All viral strains were activated with trypsin and grown as described
316 (19).

317

318 **HAstV-1 CP core production**. cDNA corresponding to HAstV-1 capsid protein residues 80
319 to 429 (accession number AAC34717.1) was cloned into pET52b in frame with a C-
320 terminal thrombin cleavage site and a 10-histidine purification tag sequence. The
321 plasmid was transformed into Escherichia coli strain BL21(DE3)pLysS, and HAstV-1 CP
322 core expression was induced with 1 mM IPTG (isopropyl-β-d-thiogalactopyranoside) at
323 18°C for 16 h. E. coli cells were lysed by ultrasonication in 20 mM Tris, pH 7.5, 1 M NaCl,
324 5% (vol/vol) glycerol, 1 mM dithiothreitol (DTT), and 20 mM imidazole containing 2 µM
325 $MgCl_2$, 1,250 U Benzonase (Millipore), and 1× protease inhibitor cocktail Set V EDTA-
326 Free (Millipore). The HAstV-1 CP core was purified from soluble lysates by HisTrap
327 metal-affinity chromatography. The HAstV-1 CP core was further purified by size-
328 exclusion chromatography on a Superdex 75 column in 20 mM phosphate buffer, pH
329 7.6, 1 M NaCl, and 5% (vol/vol) glycerol.
330
331 **HAstV spike production.** Synthetic genes codon optimized for *Escherichia coli* encoding
332 HAstV-2-Oxford amino acids 431 to 674 capsid spike (GenBank accession number
333 KY964327), HAstV-1 capsid protein residues 429 to 645 (accession number AAC34717.1),
334 or HAstV-8 CP spike amino acids 429 to 647 (UniProtKB entry Q9IFX1). To make spike
335 expression plasmids, genes were cloned into pET52b (Addgene) in frame with a C-
336 terminal thrombin cleavage site and a 10-histidine purification tag. All plasmids were
337 verified by DNA sequencing. Plasmids were transformed into *E. coli* strain BL21(DE3),
338 and protein production was induced with 1 mM IPTG at 18°C for 16 h. *E. coli* cells were
339 lysed by ultrasonication in 20 mM Tris-HCl (pH 8.0), 500 mM NaCl, and 20 mM imidazole

containing 2 μM $MgCl_2$, 1,250 U Benzonase (Millipore), and 1× protease inhibitor cocktail Set V EDTA-Free (Millipore). Proteins were purified from soluble lysates by HisTrap metal-affinity chromatography. Proteins were buffer exchanged into PBS and further purified by size exclusion chromatography on a Superdex 200 column in PBS.

Polyclonal sera production. Rabbit anti-spike1 polyclonal serum was generated by immunization of New Zealand rabbits with 250 μg of recombinant HAstV-1 capsid spike in Freund's complete adjuvant (FCA) followed by three immunizations, every two weeks, with 250 μg of the protein in Freund's incomplete adjuvant (FIA). Rabbit anti-core1 polyclonal serum and rabbit anti-HAstV-8 have been previously described (19). Mouse polyclonal sera to either spikes 1, 2, or 8 were generated by immunization of BALB/c mice with 50 μg of the corresponding recombinant protein in FCA, followed by three immunizations, every two weeks, with 50 μg of the same protein in FIA.

Monoclonal antibody production. Eight-week-old BALB/c mice were immunized with 50 μg of spike1 recombinant protein 1:1 with FCA, three more immunizations were performed every two weeks using a mix containing 50 μg of each, spike1, spike2 and spike8 1:1 in FIA. Four days after the last immunization the spleen was isolated and splenocytes were fused with Fox myeloma cells using 50% polyethylene glycol; the cells were suspended in HAT (hypoxanthine- aminopterin-thymidine) medium and directly plated in 96-well plates. Hybridomas secreting antibodies to either recombinant spike (1, 2, or 8) were screened by an ELISA (see below), and those positive by the ELISA test

were then assayed in a neutralization assay (see below). The hybridomas of interest were cloned three times by limiting dilution using thymocyte feeder layers. Selected MAbs were amplified as mouse ascites.

ELISA. Purified spike proteins at a concentration of 2 µg/mL in PBS (50 µL total) were incubated 1 h at 37°C in 96-well ELISA microtiter plates. The plates were then washed three times with PBS containing 0.1% Tween 20 (PBST). The wells were blocked by adding 100 µL of 1% BSA in PBS and incubating at 37°C for 1 h, followed by three PBST washes. Conditioned medium from the hybridoma cells or the indicated dilution of mouse or rabbit polyclonal sera was added and incubated at 37°C for 1 h, and then washed three times with PBST. Plates were incubated for 1 h at room temperature with 50 µL of goat anti-mouse antibody conjugated to alkaline phosphatase (KPL) diluted 1:1,000 in PBS, or goat anti-rabbit antibody conjugated to alkaline phosphatase (KPL) diluted 1:1,000 in PBS. The plates were washed three times with PBST and the reaction was developed by adding the phosphatase substrate (Sigma 104 at 1 mg/ml) diluted in diethanolamine buffer (100 mM diethanolamine [pH 9.4], 1 mM $MgCl_2$, 5 mM sodium azide). The absorbance was recorded at 405 nm in a FLUOstart Omega (BMG Labtech).

Neutralization assays. The indicated concentration of antibody was pre-incubated at an MOI of 0.002 of the indicated HAstV strain for 1 h at room temperature. The virus-antibody mixture was then added to confluent C2Bbe1 cell monolayers grown in 96-well plates, and incubated for 1 h at 37°C. After this time, the cells were washed three times

384 with minimum essential medium (MEM) without serum, and the infection was left to
385 proceed for 18 h at 37°C. Infected cells were detected by an immunoperoxidase focus-
386 forming assay, as described (19). The neutralization antibody titer was defined as the
387 antibody dilution that blocks at least 50% of the input virus.
388
389 **Sequencing.** To determine the nucleotide sequence of the various HAstV spikes, RNA
390 was isolated from viral lysates using PureLink® viral RNA/DNA Mini Kit (Invitrogen).
391 cDNA was then synthesized with SuperScript™ III reverse transcriptase (Thermo Fisher
392 Scientific) using the following primers: 5'-CGGCTTCCAGATGTGCAG-3' (HAstV-1Lw)
393 corresponding to nucleotides 6658-6675 of the HAstV-1 strain Oxford (accession
394 number L23513.1); 5'-GCGGTCTCCAGAAAGTTTG-3' (HAstV-2Lw) corresponding to
395 nucleotides 2369-2387 of the HAstV-2 strain Oxford (accession number 8497068); or 5'-
396 GCTTCCAGATAGTTGCAG-3' (HAstV-8Lw) corresponding to the nucleotides 6639-6656 of
397 the HAstV-8 strain Yuc8 (accession number AF260508.1). For PCR amplification, Vent®
398 DNA Polymerase (New England BioLabs) was used, with the following primers: HAstV-
399 2Up, 5'-CAGTTCACTCAAATGAACCA-3', corresponding to nucleotides 1215 to 1234 of the
400 HAstV-2 capsid gene (accession number L06802.1), were used for HAstV-1-RIVMb and
401 HAstV-2-Oxford strains, and primer HAstV-8Up, 5'-CAGTTTACACAGATGAATCA-3',
402 corresponding to nucleotides 5531-5551 of the HAstV-8 strain Yuc8 (accession number
403 AF260508.1), for HAstV-8-Yuc8. The PCR product was purified using the DNA clean and
404 Concentrator-5 kit (Zymo Research) and sequenced using the Sanger chemistry in the
405 sequencing facility of the Instituto de Biotecnología, UNAM. The sequences of the

406 amplified PCR products were deposited in GenBank, with accession numbers MH763691
407 (HAstV-1), KY964327 (HAstV-2), and MH763692 (HAstV-8).
408
409 **Isolation of neutralization escape variants.** For selection of escape variants, we
410 incubated viral lysates (with at least 1 X 10^7 ffu/ml) with the appropriate mAb at
411 1:1,000-1:100 dilution of the ascites fluid for 1 h at room temperature, then the mix was
412 used to infect CaCo-2 monolayers grown in 6-well plates for 1 h at 37°C, and the
413 unbound virus was removed by washing three times. The cell monolayers were
414 incubated at 37°C by 48 to 72 hpi in the presence of trypsin (5 µg/ml), tetracycline (1
415 µg/ml), and the corresponding mAb diluted 1:1,000. Viral lysates were then prepared by
416 three cycles of freeze-thawing, and the procedure was repeated for at least three times
417 before confirming the phenotype. The phenotype of the variant viruses was evaluated
418 by neutralization assays, and the selection was repeated until detection of the
419 neutralization escape variant (this usually took 4 to 5 passages in the presence of the Nt-
420 MAb). The double-escape variants were selected as described above, but starting with
421 the single variant, instead of the wt virus.
422
423 **ACKNOWLEDGMENTS**
424 This work was partially supported by grants from DGAPA/UNAM [IG200317] and
425 [IN208317], and the National Council for Science and Technology-Mexico (CONACYT)
426 [A1-S-9477]. This work was also supported by the National Institutes of Health, National
427 Institute of Allergy and Infectious Diseases grant AI130073 (to R.M.D.).

REFERENCES

1. **Bosch A, Pinto RM, Guix S.** 2014. Human astroviruses. Clin Microbiol Rev **27:**1048-1074.
2. **Cortez V, Freiden P, Gu Z, Adderson E, Hayden R, Schultz-Cherry S.** 2017. Persistent Infections with Diverse Co-Circulating Astroviruses in Pediatric Oncology Patients, Memphis, Tennessee, USA. Emerg Infect Dis **23:**288-290.
3. **Méndez E, Arias CF.** 2013. Astroviruses, p 1347-1401. *In* Knipe DMH, P.M. (ed), Fields Virology, 6th ed, vol 1. Lippincot Williams & Wilkins, Philadelphia, PA.
4. **Vu DL, Bosch A, Pinto RM, Guix S.** 2017. Epidemiology of Classic and Novel Human Astrovirus: Gastroenteritis and Beyond. Viruses **9**.
5. **Olortegui MP, Rouhani S, Yori PP, Salas MS, Trigoso DR, Mondal D, Bodhidatta L, Platts-Mills J, Samie A, Kabir F, Lima A, Babji S, Shrestha SK, Mason CJ, Kalam A, Bessong P, Ahmed T, Mduma E, Bhutta ZA, Lima I, Ramdass R, Moulton LH, Lang D, George A, Zaidi AKM, Kang G, Houpt ER, Kosek MN, Network M-E.** 2018. Astrovirus Infection and Diarrhea in 8 Countries. Pediatrics **141**.
6. **Platts-Mills JA, Babji S, Bodhidatta L, Gratz J, Haque R, Havt A, McCormick BJ, McGrath M, Olortegui MP, Samie A, Shakoor S, Mondal D, Lima IF, Hariraju D, Rayamajhi BB, Qureshi S, Kabir F, Yori PP, Mufamadi B, Amour C, Carreon JD, Richard SA, Lang D, Bessong P, Mduma E, Ahmed T, Lima AA, Mason CJ, Zaidi AK, Bhutta ZA, Kosek M, Guerrant RL, Gottlieb M, Miller M, Kang G, Houpt ER, Investigators M-EN.** 2015. Pathogen-specific burdens of community diarrhoea in

developing countries: a multisite birth cohort study (MAL-ED). Lancet Glob Health **3:**e564-575.

7. **Arias CF, DuBois RM.** 2017. The Astrovirus Capsid: A Review. Viruses **9**.

8. **Aguilar-Hernandez N, Lopez S, Arias CF.** 2018. Minimal capsid composition of infectious human astrovirus. Virology **521:**58-61.

9. **Dryden KA, Tihova M, Nowotny N, Matsui SM, Mendez E, Yeager M.** 2012. Immature and mature human astrovirus: structure, conformational changes, and similarities to hepatitis E virus. J Mol Biol **422:**650-658.

10. **Toh Y, Harper J, Dryden KA, Yeager M, Arias CF, Mendez E, Tao YJ.** 2016. Crystal Structure of the Human Astrovirus Capsid Protein. J Virol **90:**9008-9017.

11. **York RL, Yousefi PA, Bogdanoff W, Haile S, Tripathi S, DuBois RM.** 2015. Structural, Mechanistic, and Antigenic Characterization of the Human Astrovirus Capsid. J Virol **90:**2254-2263.

12. **Bogdanoff WA, Campos J, Perez EI, Yin L, Alexander DL, DuBois RM.** 2017. Structure of a Human Astrovirus Capsid-Antibody Complex and Mechanistic Insights into Virus Neutralization. J Virol **91**.

13. **Dong J, Dong L, Mendez E, Tao Y.** 2011. Crystal structure of the human astrovirus capsid spike. Proc Natl Acad Sci U S A **108:**12681-12686.

14. **DuBois RM, Freiden P, Marvin S, Reddivari M, Heath RJ, White SW, Schultz-Cherry S.** 2013. Crystal structure of the avian astrovirus capsid spike. J Virol **87:**7853-7863.

15. **Bass DM, Qiu S.** 2000. Proteolytic processing of the astrovirus capsid. J Virol

74:1810-1814.

16. **Sanchez-Fauquier A, Carrascosa AL, Carrascosa JL, Otero A, Glass RI, Lopez JA, San Martin C, Melero JA.** 1994. Characterization of a human astrovirus serotype 2 structural protein (VP26) that contains an epitope involved in virus neutralization. Virology **201:**312-320.

17. **Bass DM, Upadhyayula U.** 1997. Characterization of human serotype 1 astrovirus-neutralizing epitopes. J Virol **71:**8666-8671.

18. **Giammarioli AM, Mackow ER, Fiore L, Greenberg HB, Ruggeri FM.** 1996. Production and characterization of murine IgA monoclonal antibodies to the surface antigens of rhesus rotavirus. Virology **225:**97-110.

19. **Bogdanoff WA, Perez EI, Lopez T, Arias CF, DuBois RM.** 2018. Structural Basis for Escape of Human Astrovirus from Antibody Neutralization: Broad Implications for Rational Vaccine Design. J Virol **92**.

FIGURE LEGENDS

Figure 1. Immunogenicity and induction of neutralizing antibodies by recombinant HAstV capsid core and spike domains. A) Recombinant capsid core and spike domains of HAstV serotype 1 (core1 and spike1) were immobilized on ELISA plates and then incubated with the indicated dilution of rabbit preimmune (PI) or hyperimmune (HI) polyclonal sera (Anti-core1 and Anti-spike1). The interaction was determined as described in Material and Methods, and the optical density (OD) of the developed color was detected at 405 nm. Experiments were performed in biological duplicates carried out in duplicate. The data were normalized to the maximal OD obtained in each experiment and represent the mean ± SEM. The maximal OD_{405} for the anti-spike1 serum was 2.49 and 2.39 for anti-core1. B) The indicated HAstV strains were preincubated with the HI rabbit sera directed to either the core1 or spike1 proteins at the indicated dilutions, and the infectivity of the viruses was determined as described in Material and Methods. All the infectivity experiments were performed in biological triplicates carried out in duplicate. The data are expressed as percentage of the positive control (viruses not incubated with antibodies), and represent the mean ± SEM.

Figure 2. Interaction of anti-spike polyclonal antibodies with recombinant spikes by ELISA and anti-core polyclonal antibodies with viral proteins by immunofluorescence and Western blot. Recombinant spikes derived from HAstV serotypes 1, 2, or 8 were immobilized in ELISA plates and they were later incubated with the indicated dilution of mouse anti-spike1 (A), anti-spike2 (B) or anti-spike8 (C) antibodies. The interaction was

508 determined as described in Material and Methods, and the optical density (OD) of the
509 color developed was detected at 405 nm. Experiments were performed in biological
510 triplicates carried out in duplicate. The data were normalized to the maximal OD
511 obtained in each experiment and represent the mean ± SEM. The maximal OD_{405} for the
512 anti-spike1 serum was 2.77; 2.91 for the anti-spike2; and 2.87 for anti-spike8. (D) Caco-2
513 cells were infected with either HAstV serotypes 1, 2, or 8 at an MOI of 0.08, and at 20
514 hpi were fixed with formaldehyde and incubated with anti-core1 polyclonal antibodies
515 at a 1:200 dilution. The cells were subsequently incubated with Alexa 488-labeled anti-
516 IgG antibodies and observed for immunofluorescence. (E) Caco-2 cells were infected
517 with either HAstV serotypes 1, 2, or 8 at an MOI of 0.3, and at 20 hpi were lysed and the
518 viral proteins were analyzed by Western blot, using anti-core1 polyclonal antibodies at a
519 1:500 dilution followed by incubation with Alexa 647-labeled anti-IgG antibodies and
520 detected in a Typhoon FLA 9500.
521
522 **Figure 3.** Specificity of neutralizing monoclonal antibodies. HAstV serotypes 1, 2, or 8
523 were pre-incubated with MAbs 3B4 (A), 3H4 (B), 4B6 (C), 2D9 (D), or 3E8 (E), or with
524 mouse hyperimmune (HI) polyclonal sera directed to the indicated spike proteins (F), at
525 the indicated dilutions. The infectivity of the viruses was determined as described in
526 Material and Methods. All experiments were performed in biological triplicates carried
527 out in duplicate. The data are expressed as percentage of the positive control (viruses
528 not incubated with antibodies), and represent the mean ± SEM.
529

Figure 4. Neutralization of HAstV escape variants. Escape variants vHAstV-1/3B4 (A), vHAstV-1/3H4 (B), vHAstV-2/4B6 (D), vHAstV-8/2D9 (D), or vHAstV-8/3E8 (E), were pre-incubated with mouse hyperimmune (HI) polyclonal sera, or with monoclonal antibodies, at the indicated dilutions. The infectivity of the viruses was determined as described in Material and Methods. All experiments were performed in biological triplicates carried out in duplicate. The data are expressed as percentage of the positive control (viruses not incubated with antibodies), and represent the mean ± SEM.

Figure 5. Neutralization of double-escape variants. Double escape variants vHAstV-1/3B4/3H4 (A), vHAstV-1/3H4/3B4 (B), vHAstV-8/2D9/3E8 (C), or vHAstV-8/3E8/2D9 (D) were pre-incubated with mouse hyperimmune (HI) polyclonal sera, or with monoclonal antibodies, at the indicated dilutions. The infectivity of the viruses was determined as described in Material and Methods. All experiments were performed in biological triplicates carried out in duplicate. The data are expressed as percentage of the positive control (viruses not incubated with antibodies), and represent the mean ± SEM.

Figure 6. Localization of point mutations that confer escape to neutralization by monoclonal antibodies. A) Sequence alignment of HAstV-1-8 CP spike domains. Conserved, similar, and nonconserved amino acids are colored red, pink, and black, respectively. The amino acid residues that changed in the variants that escaped neutralization by MAbs 3H4 and 3B4 to HAstV-1, 4B6 to HAstV-2, and 3E8 and 2D9 to HAstV-8, are indicated with green, gold, and blue arrows, respectively. B) Spike1

552 structure shown from the top and one side. One half of the dimer is gray, and the other
553 half is white. The positions of the mutations that confer escape to neutralization by the
554 various monoclonal antibodies are colored green for HAstV-1, gold for HAstV-2, and blue
555 to HAstV-8. The mutations are shown in only one protomer in the dimer.
556
557

TABLES

Table 1. Characteristics of the antibodies described in this work.

Monoclonal antibody	Virus recognized	[1]Peroxidase/IF	[2]Neutralization titer
3H4	HAstV1	+	1/20,000
3B4	HAstV1	+	1/16,000
4B6	HAstV2	+	1/800,000
2D9	HAstV8	+	1/5,000,000
3E8	HAstV8	+	1/1,000,000
Polyclonal serum			
Anti-spike1	HAstV1	+	1/250,000
Anti-spike2	HAstV2	+	1/250,000
Anti-spike8	HAstV8	+	1/63,000
Anti-Core1	HAstV1 HAstV2 HAstV8	+ + +	Not neutralizing

[1]Reactivity of antibodies by immunocytochemistry and immunofluorescence, in cells infected with the indicated viruses.

562 [2]Reciprocal of the antibody dilution that reduces at least 50% of the infectious virus foci

563 of the indicated viruses in the neutralization assay described in Material and Methods.

564

565

566

567 Table 2. Position of mutations in the escape variants

Virus	Monoclonal antibody	Nt-escape variant	Amino acids changed
HAstV-1	3H4	vHAstV-1/3H4	K504E
HAstV-1	3B4	vHAstV-1/3B4	S560P
HAstV-1	3H4/3B4	vHAstV-1/3H4/3B4	K504E/S560P
HAstV-1	3B4/3H4	vHAstV-1/3B4/3H4	K504E/S560P
HAstV-2	4B6	vHAstV-2/4B6	D564E, N565D
HAstV-8	3E8	vHAstV-8/3E8	Y464H
HAstV-8	2D9	vHAstV-8/2D9	D597Y
HAstV-8	2D9/3E8	vHAstV-8/2D9/3E8	Y464H/D597Y
HAstV-8	3E8/2D9	vHAstV-8/3E8/2D9	Y464H/D597Y

568

Fig. 1

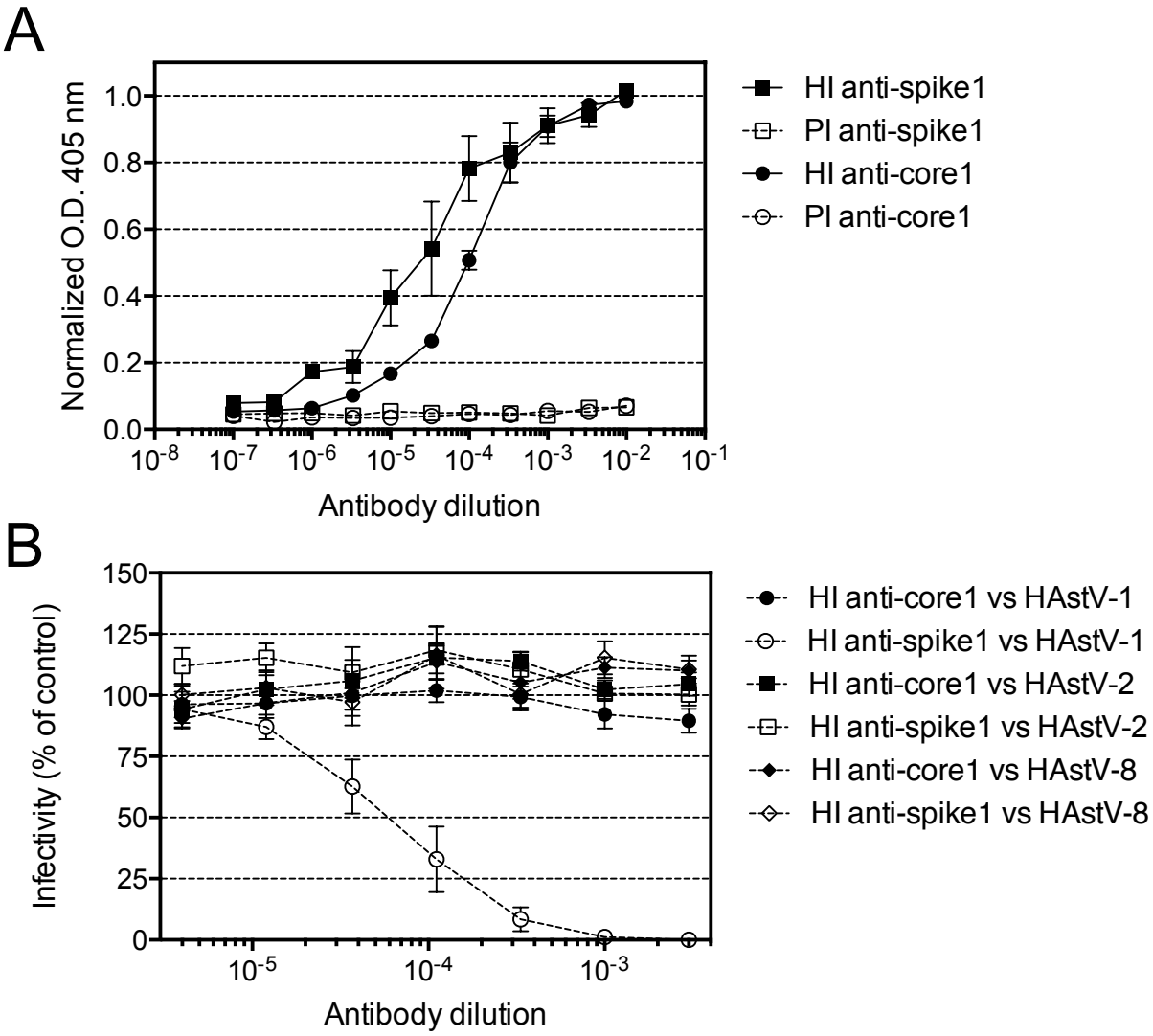
A
Normalized O.D. 405 nm
1.0
0.8
0.6
0.4
0.2
0.0
10-8
10-7
10-6
10-5
10-4
10-3
10-2
10-1
Antibody dilution
HI anti-spike1
PI anti-spike1
HI anti-core1
PI anti-core1
B
Infectivity (% of control)
150
125
100
75
50
25
0
10-5
10-4
10-3
Antibody dilution
HI anti-core1 vs HAstV-1
HI anti-spike1 vs HAstV-1
HI anti-core1 vs HAstV-2
HI anti-spike1 vs HAstV-2
HI anti-core1 vs HAstV-8
HI anti-spike1 vs HAstV-8

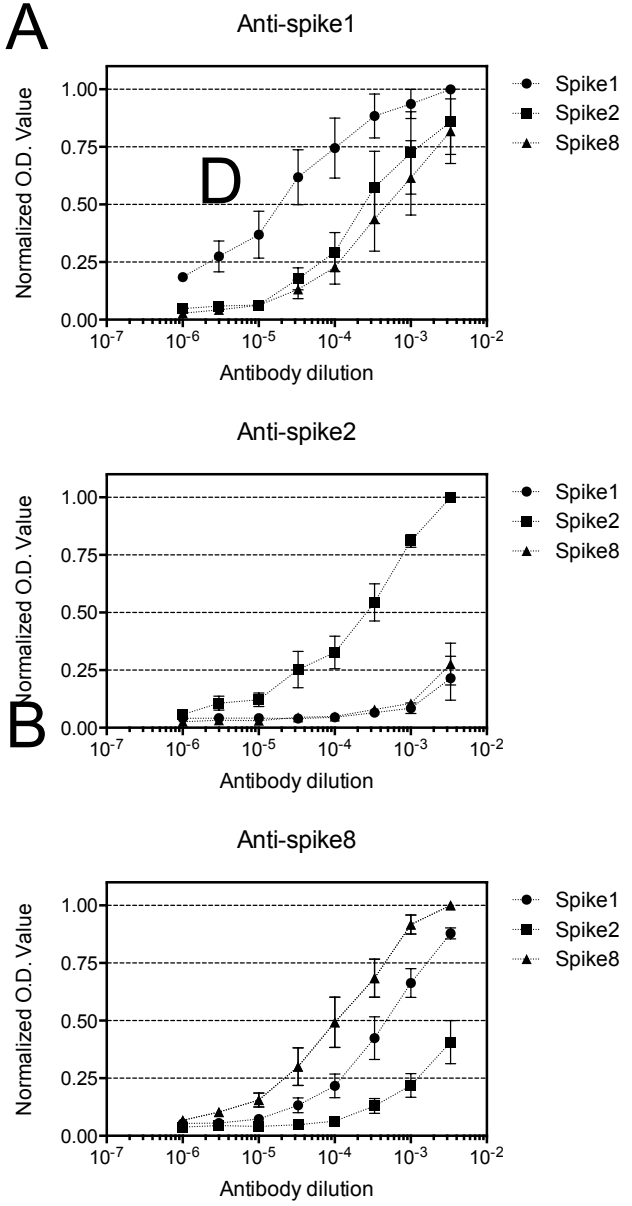
A
Anti-spike1
Normalized O.D. Value
1.00
0.75
0.50
0.25
0.00
D
Spike1
Spike2
Spike8
10^{-7} 10^{-6} 10^{-5} 10^{-4} 10^{-3} 10^{-2}
Antibody dilution
Anti-spike2
B
Anti-spike8
C

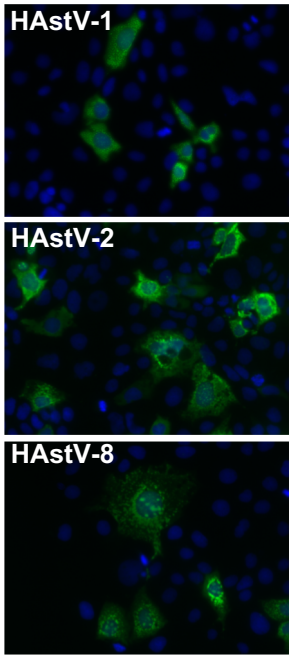
HAstV-1
HAstV-2
HAstV-8

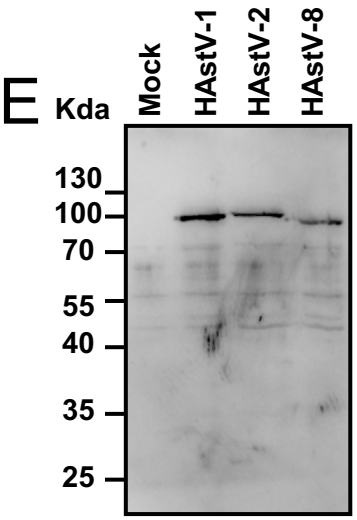
E
Kda
Mock
HAstV-1
HAstV-2
HAstV-8
130
100
70
55
40
35
25

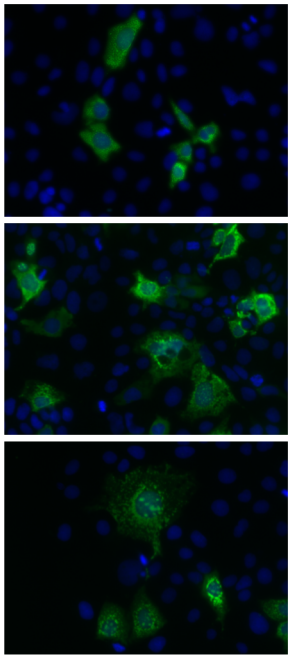

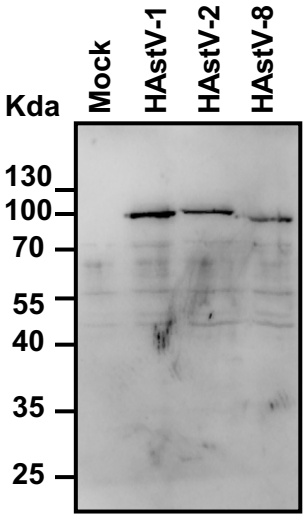
Kda
Mock
HAstV-1
HAstV-2
HAstV-8
130
100
70
55
40
35
25

Fig. 4

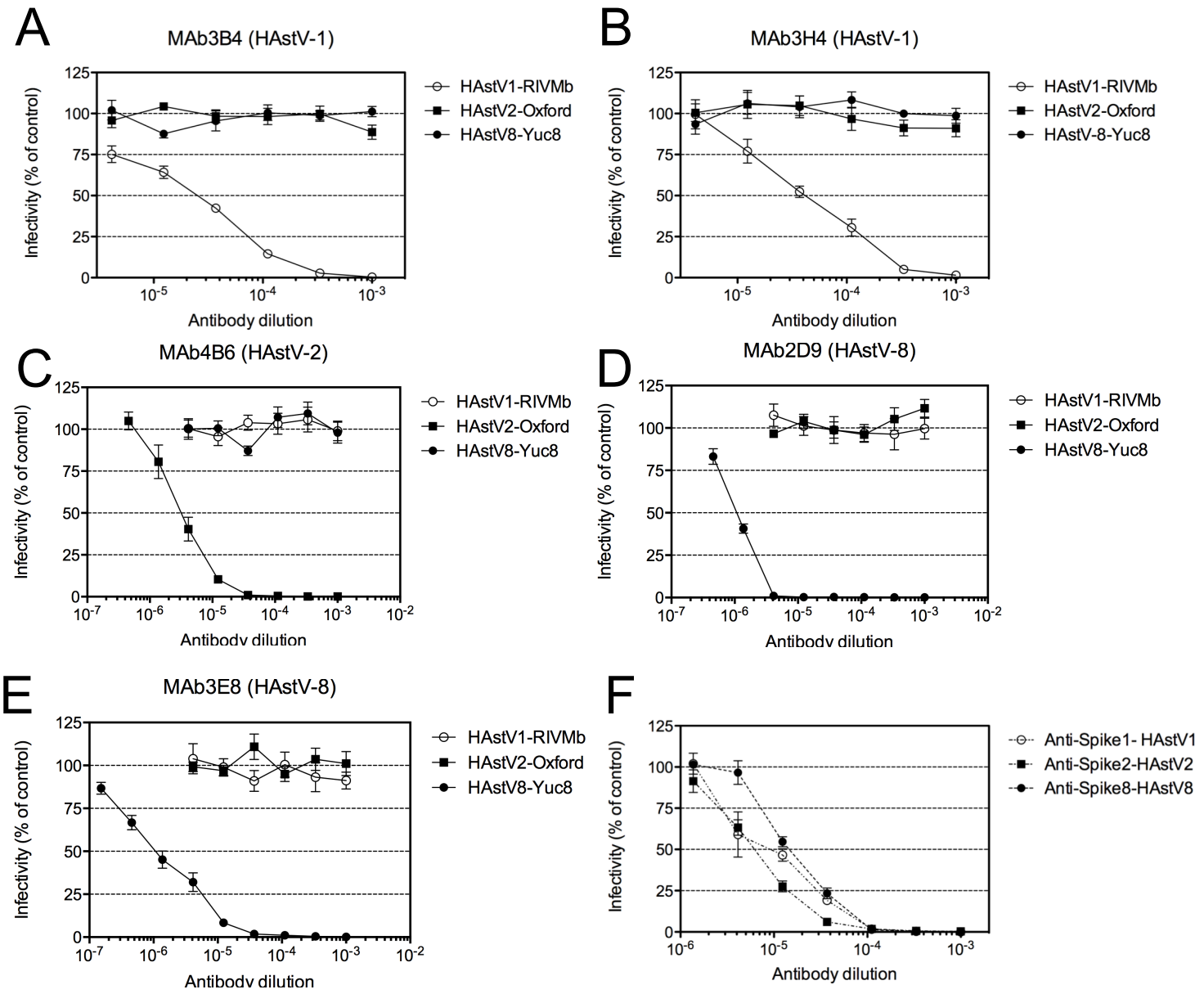
A
MAb3B4 (HAstV-1)
Infectivity (% of control)
Antibody dilution
HAstV1-RIVMb
HAstV2-Oxford
HAstV8-Yuc8
B
MAb3H4 (HAstV-1)
Infectivity (% of control)
Antibody dilution
HAstV1-RIVMb
HAstV2-Oxford
HAstV-8-Yuc8
C
MAb4B6 (HAstV-2)
Infectivity (% of control)
Antibody dilution
HAstV1-RIVMb
HAstV2-Oxford
HAstV8-Yuc8
D
MAb2D9 (HAstV-8)
Infectivity (% of control)
Antibody dilution
HAstV1-RIVMb
HAstV2-Oxford
HAstV8-Yuc8
E
MAb3E8 (HAstV-8)
Infectivity (% of control)
Antibody dilution
HAstV1-RIVMb
HAstV2-Oxford
HAstV8-Yuc8
F
Infectivity (% of control)
Antibody dilution
Anti-Spike1- HAstV1
Anti-Spike2-HAstV2
Anti-Spike8-HAstV8

Fig. 4

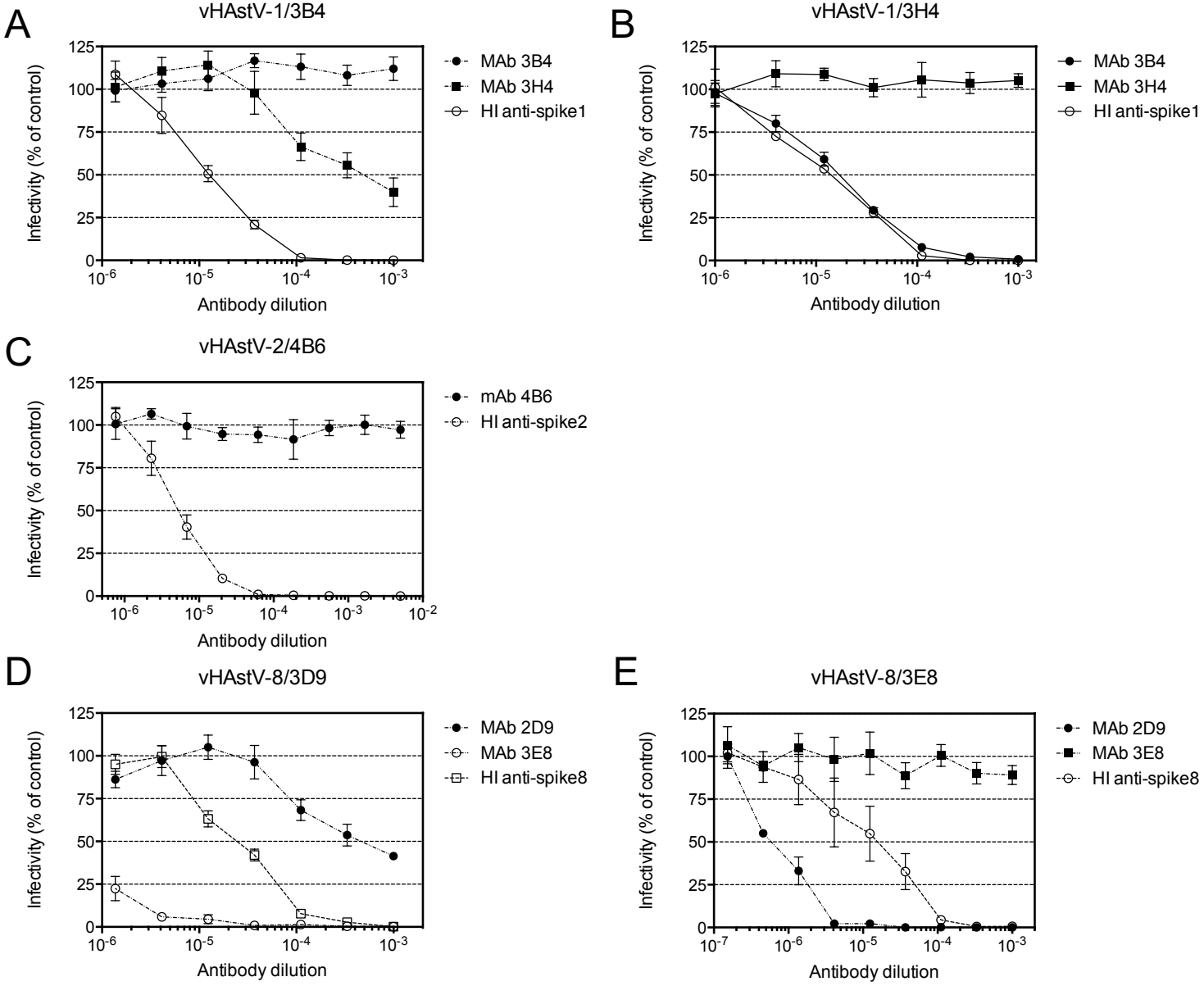
A
vHAstV-1/3B4
Infectivity (% of control)
Antibody dilution
MAb 3B4
MAb 3H4
HI anti-spike1
B
vHAstV-1/3H4
Infectivity (% of control)
Antibody dilution
MAb 3B4
MAb 3H4
HI anti-spike1
C
vHAstV-2/4B6
Infectivity (% of control)
Antibody dilution
mAb 4B6
HI anti-spike2
D
vHAstV-8/3D9
Infectivity (% of control)
Antibody dilution
MAb 2D9
MAb 3E8
HI anti-spike8
E
vHAstV-8/3E8
Infectivity (% of control)
Antibody dilution
MAb 2D9
MAb 3E8
HI anti-spike8

Fig. 5

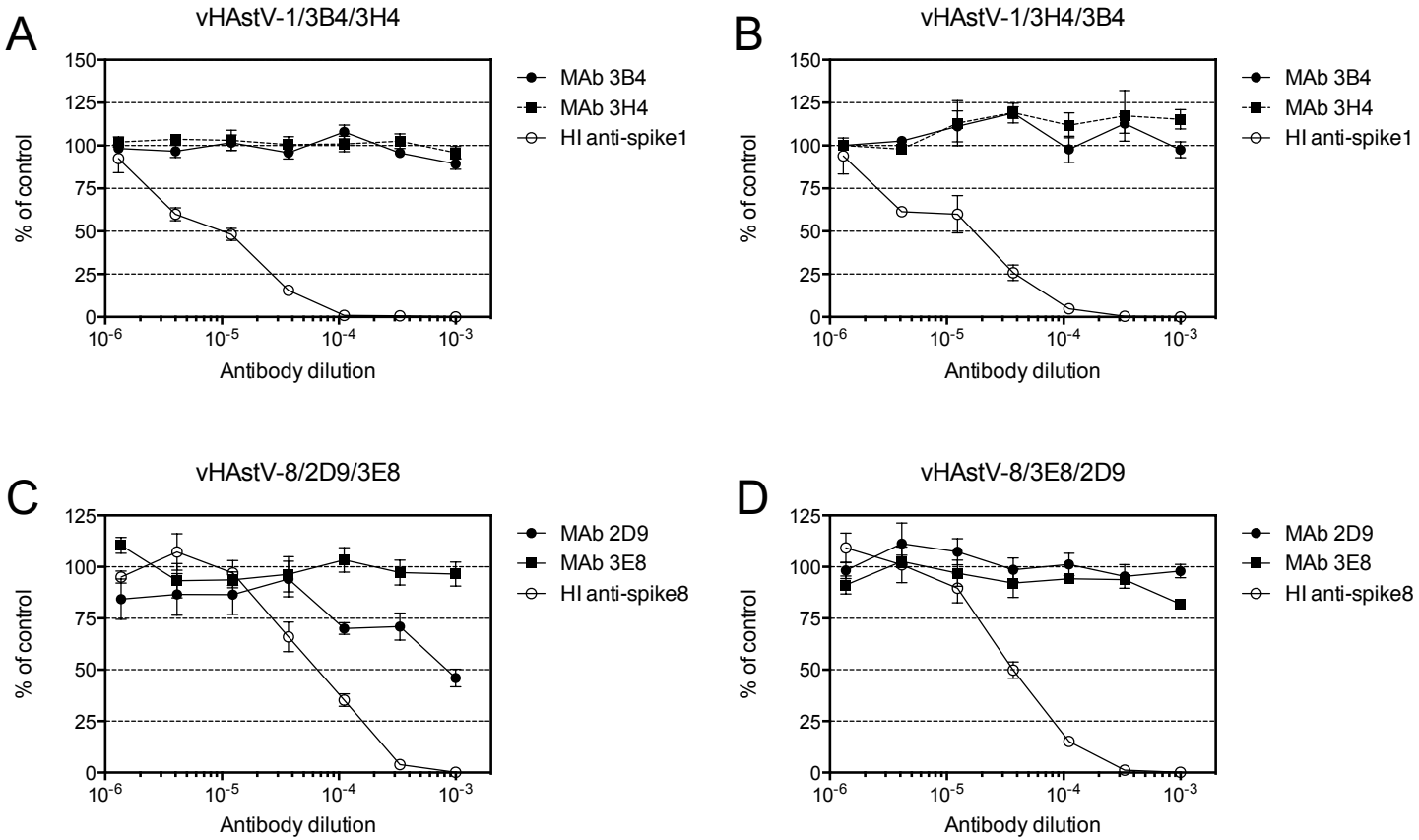
A
vHAstV-1/3B4/3H4
% of control
Antibody dilution
MAb 3B4
MAb 3H4
HI anti-spike1
B
vHAstV-1/3H4/3B4
% of control
Antibody dilution
MAb 3B4
MAb 3H4
HI anti-spike1
C
vHAstV-8/2D9/3E8
% of control
Antibody dilution
MAb 2D9
MAb 3E8
HI anti-spike8
D
vHAstV-8/3E8/2D9
% of control
Antibody dilution
MAb 2D9
MAb 3E8
HI anti-spike8

Fig. 6

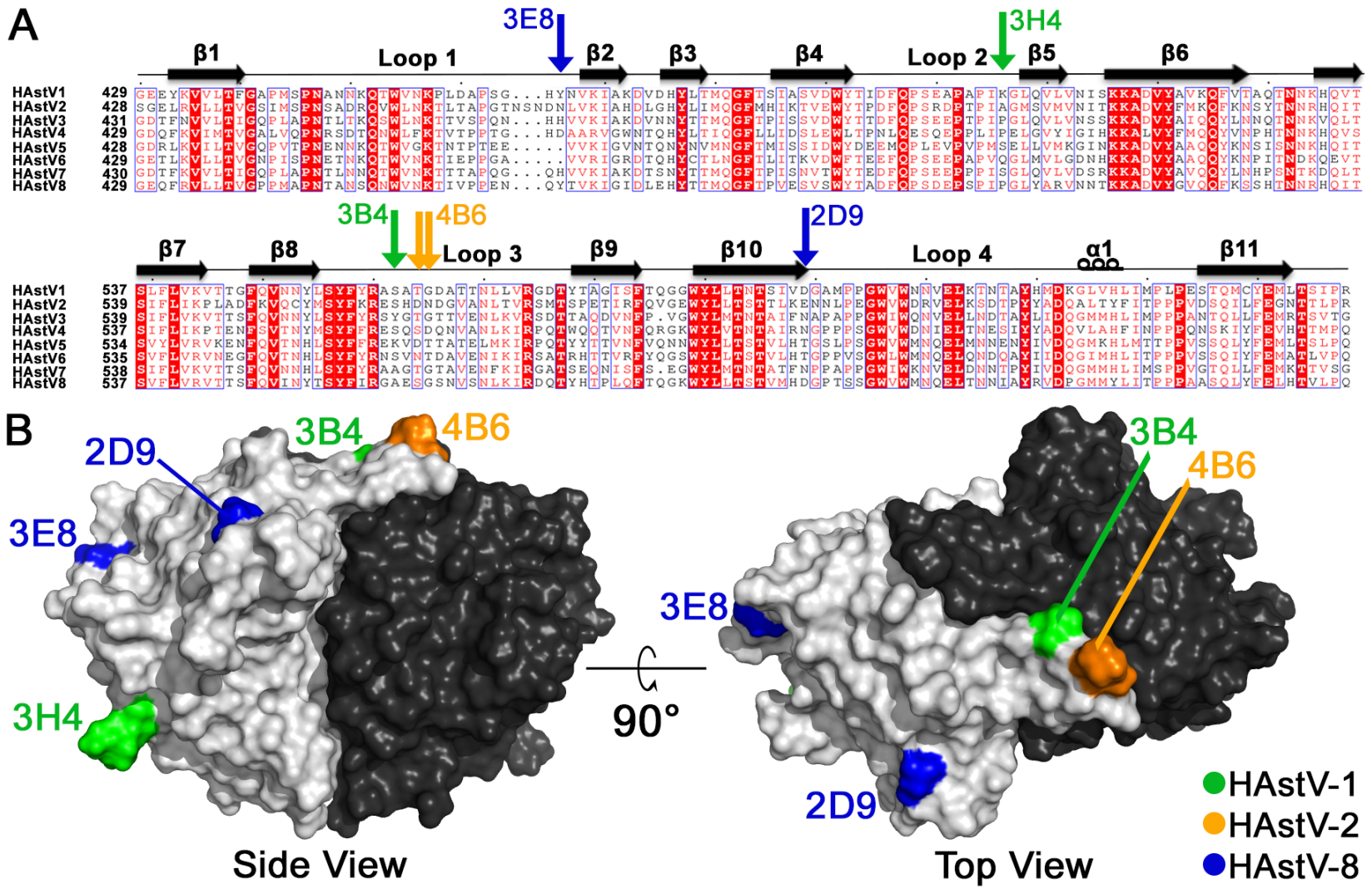
A
3E8
3H4
β1
Loop 1
β2
β3
β4
Loop 2
β5
β6
HAstV1 429
HAstV2 428
HAstV3 431
HAstV4 429
HAstV5 428
HAstV6 429
HAstV7 430
HAstV8 429
3B4
4B6
2D9
β7
β8
Loop 3
β9
β10
Loop 4
α1
β11
HAstV1 537
HAstV2 539
HAstV3 539
HAstV4 537
HAstV5 534
HAstV6 535
HAstV7 538
HAstV8 537
B
2D9
3B4
4B6
3E8
3H4
Side View
90°
3B4
4B6
3E8
2D9
Top View
HAstV-1
HAstV-2
HAstV-8